

Charge qubits in semiconductor quantum computer architectures: Tunnel coupling and decoherence

Xuedong Hu

Department of Physics, University at Buffalo, the State University of New York, Buffalo, NY 14260-1500

Belita Koiller

Instituto de Física, Universidade Federal do Rio de Janeiro, 21945, Rio de Janeiro, Brazil

S. Das Sarma

Condensed Matter Theory Center, Department of Physics,
University of Maryland, College Park, MD 20742-4111

(dated: December 23, 2021)

We consider charge qubits based on shallow donor electron states in silicon and coupled quantum dots in GaAs. Specifically, we study the feasibility of P_2^+ charge qubits in Si, focusing on single qubit properties in terms of tunnel coupling between the two phosphorus donors and qubit decoherence caused by electron-phonon interaction. By taking into consideration the multi-valley structure of the Si conduction band, we show that inter-valley quantum interference has important consequences for single-qubit operations of P_2^+ charge qubits. In particular, the valley interference leads to a tunnel-coupling strength distribution centered around zero. On the other hand, we find that the Si band structure does not dramatically affect the electron-phonon coupling and consequently, qubit coherence. We also critically compare charge qubit properties for SiP_2^+ and GaAs double quantum dot quantum computer architectures.

PACS numbers: 71.55.Cn, 03.67.Lx, 85.35.-p

I. INTRODUCTION

Among the solid state candidates for qubits in quantum information processing, semiconductor-based systems have been among the most extensively explored. Key features in favor of these proposals are the high level of theoretical understanding, experimental control, and nanofabrication capabilities currently available for semiconductors. It is commonly believed that group-IV or III-V semiconductor nanostructure-based quantum computer architectures should be relatively easily scalable because of the existence of the vast semiconductor microelectronics infrastructure. This scalability incentive has led to a great deal of recent activities in studying qubit properties of semiconductor nanostructures.^{1,2} Theoretically, many semiconductor-based quantum computers were conceived to rely on either electron spins or nuclear spins as qubits.^{3,4,5,6,7,8,9,10} Spin-1/2 fermions (electrons or nuclei) probably constitute the most natural and robust choices of quantum two-level systems for qubits in solids. Unfortunately, and in spite of considerable recent progress,^{11,12} it is difficult to perform fast measurements of single electron (or nuclear) spins, which are required for practical quantum computing implementations incorporating quantum error corrections. The problem here is quantitative (although the electron spin is surely a quantum two-level system, the Bohr magneton is a very small quantity, (and spin usually does not couple strongly to external probes), making it difficult to manipulate and measure the microscopic single spin states in the solid state environment.

In contrast to spin qubits, charge qubits in semiconductors have the substantial advantage of being easy to manipulate and measure since the experimental techniques for measuring single electron charges in semiconductors are extremely well-developed. The price one pays for the relative ease in the manipulation and read-out of single-charge states is, of course, the strong decoherence and the rather short decoherence time of the orbital charge states because they couple strongly to the environment through the long-range Coulomb interaction. This fast decoherence of orbital states makes semiconductor charge qubits rather unlikely candidates for a scalable quantum computer architecture. However, the strong interactions make the orbital states an excellent choice for studying qubit dynamics and qubit coupling in the solid state nanostructure environment. This is particularly true in view of the difficulties encountered in the manipulation and the measurement of the single spin states in semiconductors. It is worthwhile also to remember that the much-studied superconducting-Cooper-pair-box-based quantum computer architectures are charge-based systems as well,^{13,14} and there are conceptual and formal overlaps between semiconductor charge qubits and superconductor charge qubits, providing further impetus for studying orbital qubits in semiconductor nanostructures.

There have been several proposals for orbital/charge qubits in semiconductors.^{15,16,17,18,19,20} In this work we theoretically analyze single charge qubit properties for phosphorus donor states in silicon, comparing it critically with charge qubit states in coupled quantum dots (QD) in GaAs. Our specific goal is to investigate how the peculiar six-fold

valley degeneracy of Si conduction band affects the single qubit properties of orbital states in P-doped Si system. The issue is important in the context of our earlier results showing that quantum interference between valleys leads to a strong suppression of the exchange energy controlling the inter-qubit coupling in the electron-spin-based silicon quantum computer architecture.^{21,22} The dramatic adverse effect of the valley interference on the silicon exchange gate naturally raises the question of whether a similar valley interference effect would also strongly (and adversely) affect the charge qubit properties. We answer this question in this paper.

Successful coherent manipulation of electron orbital states in GaAs has been achieved for electrons bound to donor impurities²³ as well as electrons in double quantum dots.²⁴ There were also suggestions of directly using electron orbital states in GaAs or Si as the building blocks for quantum information processing.^{16,17,19,20} Specifically, a double QD with an electron bound in each dot or a pair of phosphorus donors that sit relatively close to each other (so as to have sizable wave function overlap) form an effective hydrogen molecule in GaAs or Si host material. Charge qubits may be defined by ionizing one of the bound electrons, thus leading to a double well potential filled with a single electron: The single electron ground state manifold, whether it is the two states localized in each of the wells or their symmetric and anti-symmetric combinations, can then be used as the two-level system forming a charge qubit.^{16,17} The advantage of such a charge qubit is that it is easy to manipulate and detect, while its disadvantage, as already mentioned above, is the generally fast charge decoherence as compared to spin.

Here we study the feasibility of the P_2^+ charge qubit in Si, focusing on single qubit properties in terms of the tunnel coupling between the two phosphorus donors (Sec.II), and charge decoherence of this system in terms of electron-phonon coupling (Sec.III). We take into consideration the multi-valley structure of the Si conduction band and explore whether valley interference could lead to potential problems or advantages with the operations of P_2^+ charge qubits, such as difficulties in the control of tunnel coupling similar to the control of exchange in two-electron systems,^{21,22} or favorable decoherence properties through vanishing electron-phonon coupling. In section IV we critically compare charge qubits based on Si- P_2^+ and GaAs double QD systems.

II. THE SYMMETRIC-ANTISYMMETRIC GAP FOR THE P_2^+ MOLECULE IN SILICON: QUBIT FIDELITY

We study the simple situation where a single electron is shared by a donor pair, constituting a P_2^+ molecule in Si. The charge qubit here consists of the two lowest energy orbital states of an ionized P_2 molecule in Si with only one valence electron in the outermost shell shared by the two P atoms. The key issue to be examined is the tunnel coupling and the resulting coherent superposition of one-electron states, rather than the entanglement among electrons, as occurs for an exchange-coupled pair of electrons.

The donors are at substitutional sites R_A and R_B in an otherwise perfect Si structure. In the absence of an external bias, and for well separated donors, we may write the eigenstates for the two lowest-energy states as a superposition of single-donor ground state wavefunctions localized at each donor, $\psi_A(r)$ and $\psi_B(r)$, similar to the standard approximation for the H_2^+ molecular ion.²⁵ The symmetry of the molecule leads to two eigenstates on this basis, namely the symmetric and antisymmetric superpositions

$$\psi_{\pm}(r) = \frac{\psi_A(r) \pm \psi_B(r)}{2(1 \pm S)}; \quad (1)$$

where $S = \int \psi_A \psi_B$ is the overlap integral and is real.²² The conduction band of bulk Si has six degenerate minima ($\ell = 1, \dots, 6$), located along the $\langle 100 \rangle$ axis of the Brillouin zone at $\mathbf{k} = \pm \frac{\pi}{a} \hat{x}$ from the Γ point, where $a = 0.357 \text{ nm}$ is the Si lattice parameter. Following Kohn-Luttinger effective mass approximation,²⁶ the single-donor ground state wavefunctions are written in terms of the six unperturbed Si band edge Bloch states $\psi_{\ell} = u(r)e^{i\mathbf{k}_{\ell} \cdot \mathbf{r}}$. For the donor at R_A ,

$$\psi_A(r) = \sum_{\ell=1}^6 F_{\ell}(r - R_A) \psi_{\ell}(r; R_A) = \sum_{\ell=1}^6 F_{\ell}(r - R_A) u_{\ell}(r) e^{i\mathbf{k}_{\ell} \cdot (r - R_A)}; \quad (2)$$

where the envelope functions centered at the donor site, $F_{\ell}(r - R_A)$, are deformed shallow donor effective mass 1S hydrogenic orbitals. For instance, for $\ell = z$, $F_z(r) = \exp[-\sqrt{(\frac{x^2 + y^2}{a^2} + \frac{z^2}{b^2})}] = \exp[-\sqrt{\frac{r^2}{a^2 b^2}}]$. The expansion coefficients, which are also called valley populations, are real.²⁷ The effective Bohr radii a and b are variational parameters chosen to minimize $E_A = \langle \psi_A | H_A | \psi_A \rangle$, leading to $a = 0.25 \text{ nm}$ and $b = 0.14 \text{ nm}$ when recently measured effective mass values are used in the minimization.²¹ The operator H_A (note that in our notation the single donor Hamiltonians H_A and H_B are equivalent) is the single-donor Hamiltonian for the bound electron,²⁸ which includes the

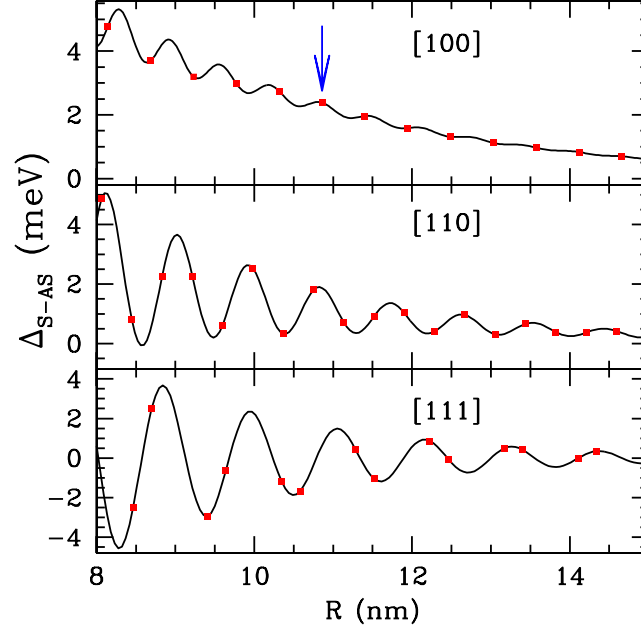


FIG. 1: (color online) Symmetric-antisymmetric gap for the P_2^+ molecular ion in Si for the donor pair along the indicated lattice directions. The arrow in the upper frame indicates the target configuration analyzed in Fig. 2.

kinetic energy, the Si periodic potential, the impurity screened Coulomb potential centered at R_A , and the valley-orbit effects, leading to $E_A \approx 40$ meV, consistent with the experimentally observed value of 45 meV.

The Hamiltonian for the singly ionized donor pair P_2^+ can then be written as

$$H = H_A - \frac{e^2}{|\mathbf{r} - \mathbf{R}_B|} + \frac{e^2}{|\mathbf{R}_A - \mathbf{R}_B|}; \quad (3)$$

from which it is straightforward to obtain the expectation value of the single qubit energy gap between the lowest-lying (symmetric and antisymmetric) states $\langle \mathbf{r} \rangle$ in (1):

$$\Delta_{S-AS} = \langle \mathbf{H} | \mathbf{j} \rangle - \langle \mathbf{H} | \mathbf{j} \rangle = \frac{2}{1 - S^2} \sum_{\mathbf{R}} X^6(\mathbf{R}) \cos(\mathbf{k} \cdot \mathbf{R}); \quad (4)$$

where $\sum_{\mathbf{R}} = \frac{1}{6} \sum_{\mathbf{R}}^{\text{P-}}$ for unstrained Si,²⁷ $X^6(\mathbf{R}) = \mathbf{j} \cdot \mathbf{j}^2 (S C_1 - v)$ and expressions for S, C_1, s and v , all of which are functions of $R = |\mathbf{R}_A - \mathbf{R}_B|$, are given in Ref. 22. For $\mathbf{R} \cdot \mathbf{j} \ll a; b, S \ll 1$, and the amplitudes $X^6(\mathbf{R})$ are monotonically decaying functions of the interdonor distance R . Except for the anisotropy, which is a consequence of the effective mass anisotropy in Si, the dependence of Δ_{S-AS} on $\mathbf{R} \cdot \mathbf{j}$ is qualitatively similar to the symmetric-antisymmetric gap in the H_2^+ molecule, namely an exponential decay with power-law prefactors. The main difference here comes from the cosine factors, which are related to the oscillatory behavior²⁸ of the donor wavefunction in Si arising from the Si conduction band valley degeneracy and to the presence of two pinning centers.

Figure 1 gives the calculated gaps as a function of R for a donor pair along three high-symmetry crystal directions. Two points are worth emphasizing here, which are manifestly different from the corresponding hydrogenic molecular ion behavior: (i) Δ_{S-AS} is an anisotropic and fast oscillatory function of R ; (ii) the sign of Δ_{S-AS} may be positive or negative depending on the precise value of R . The characteristics mentioned in point (i) are similar to the exchange coupling behavior previously discussed for the two-electrons neutral donor pair.^{21,22,28} Point (ii) implies that the P_2^+ molecular ion ground state in Si may be symmetric (as in the H_2^+ molecular ion case) or antisymmetric depending on the separation between the two P atoms. Note that for the two-electron case, the ground state is always a singlet (i.e. a symmetric two-particle spatial part of the wavefunction with the spin part being antisymmetric), implying that the

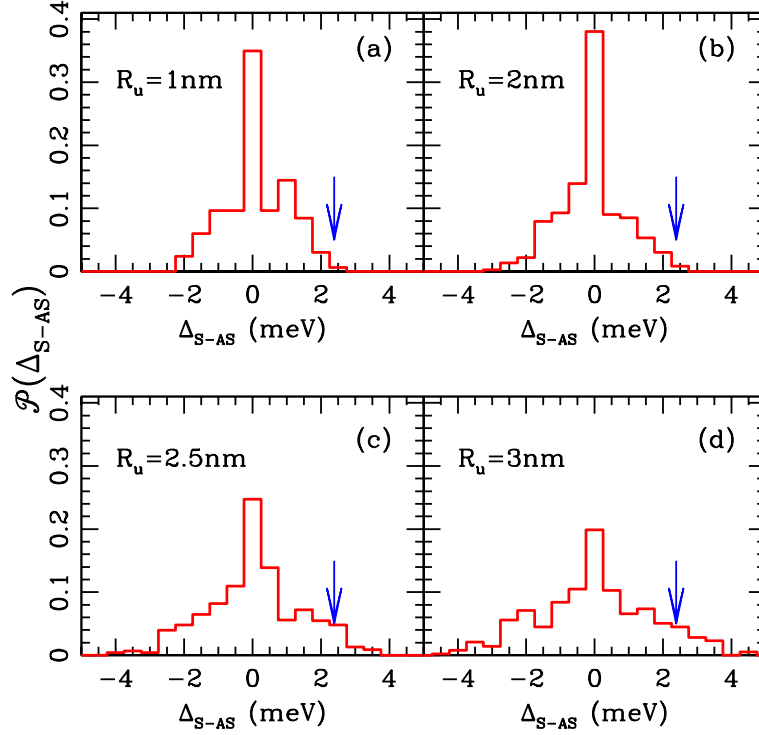


FIG. 2: (color online) Probability distributions of the symmetric-antisymmetric gap for the P_2^+ molecular ion in Si. Donor pairs are approximately aligned along [100], but with an uncertainty radius R_u with respect to this target axial alignment (see text). The arrow in each panel indicates the gap value for the target configuration, for which the uncertainty radius is $R_u = 0$. Notice that all four distributions are peaked at $\Delta_{S-AS} = 0$, and not at the target gap value.

exchange J is always positive for a two-electron molecule. For a one-electron ionized molecule, however, the ground state spatial wavefunction can be either symmetric or antisymmetric.

Figure 2 shows normalized probability distributions for the Δ_{S-AS} gap values when the first donor is kept fixed at R_A and the second donor is placed at a site 20 lattice parameters away ($\approx 108.6\text{\AA}$), along the [100] axis. This target configuration is indicated by an arrow in Fig. 1. We allow the second donor position R_B to visit all possible substitutional diamond lattice positions within a sphere of radius R_u centered at the attempted position. Our motivation here is to simulate the realistic fabrication of a P_2^+ molecular ion with fixed inter-atomic distance in Si with the state of the art Si technology, in which there will always be a small ($R_u \approx 1 - 3\text{ nm}$) uncertainty in the precise positioning of the substitutional donor atom within the Si unit cell. We would like to estimate the resultant randomness or uncertainty in Δ_{S-AS} arising from this uncertainty in R_B . For $R_u = 0$, i.e., for $R = 20a_0$, $\Delta_{S-AS} \approx 2.4\text{ meV}$, given by the arrows in Fig. 2. We incorporate the effect of small uncertainties by taking $R_u = 1\text{ nm}$, corresponding to the best reported degree of accuracy in single P atom positioning in Si.²⁹ These small deviations completely change the qubit gap distribution, as given by the histogram in Fig. 2(a) strongly peaked around zero. A similar distribution is obtained for $R_u = 2\text{ nm}$, as illustrated in Fig. 2(b). Further increasing R_u leads to broader distributions of the gap values, though still peaked at zero [see Fig. 2(c) and (d)]. This broadening is due to the fast increase in the number of lattice sites inside the sphere of radius R_u , thus contributing to the distribution, as R_u increases. We conclude that the valley interference between the six Bloch states leads to a strong suppression of the qubit delity since the most probable Δ_{S-AS} tends to be zero.

A very small Δ_{S-AS} is undesirable in defining the two states $|j_i\rangle$ and $|j_l\rangle$ forming the charge qubit. If we take them to be the symmetric and anti-symmetric states given in Eq. (1), the fact that they are essentially degenerate means that, when one attempts to initialize the qubit state at $|j_i\rangle$, a different combination $|j_i\rangle + |j_l\rangle$ might result. Well defined qubits may still be defined under a suitable applied external bias, so that the electron ground state wavefunction is localized around one of the donors, say at lattice site R_A , and the first excited state is localized around R_B .

Single qubit rotations, used to implement universal quantum gates,³⁰ might in principle be achieved by adiabatic tunneling of the electron among the two sites under controlled axially aligned electric fields through bias sweeps.³¹

When, at zero bias, the ground state is not well separated by a gap from the first excited state, severe limitations are expected in the adiabatic manipulation of the electron by applied external fields. In other words, the fidelity of the single qubit system defining the quantum two-level dynamics will be severely compromised by the valley interference effect.

III. ELECTRON-PHONON COUPLING FOR A P_2^+ MOLECULE

Two key decoherence channels for charge qubits in solids are background charge fluctuations and electron-phonon coupling.²⁴ The former is closely related to the sample quality (e.g., existences of stray charges and charged defects in the system) and is extrinsic, while the latter is intrinsic. Here we focus on the electron-phonon coupling. A critical question for the P_2^+ molecular ion in Si is whether the Si band structure and the associated charge density oscillations²⁸ lead to any significant modification of the electron-phonon coupling matrix elements. In the following, we first derive the electron-phonon coupling for a single valley situation, such as GaAs, to set a benchmark, then assess the effect of the Si conduction band valleys and the Bloch functions on the donor electron-phonon coupling matrix elements. Our motivation is to investigate whether valley interference leads to a strong suppression of the electron-phonon coupling (similar to the suppression of exchange and tunnel couplings), which would be beneficial for silicon charge qubits.

According to the results in Sec. II, the energy splitting ϵ_{SAS} between the two lowest energy states in a P_2^+ molecular ion is up to a few meV, thus only low energy acoustic phonons near the Brillouin zone center $q \approx 0$ contribute to phonon-induced electron decoherence. Electron-acoustic-phonon coupling in a semiconductor can be classified into two types: deformation potential and piezoelectric. Since Si is not polar, deformation potential is the only relevant interaction. We will thus focus on this interaction for the rest of this paper. The electron-phonon interaction takes the form:³²

$$H_{\text{ep}} = D \sum_{\mathbf{q}} \frac{\hbar}{2mV} \sum_{\mathbf{q}}^{\mathbf{1=2}} \hat{J}(\mathbf{q}) (a_{\mathbf{q}} + a_{\mathbf{q}}^\dagger); \quad (5)$$

where D is the deformation constant, m is the mass density of the host material, V is the volume of the sample, $a_{\mathbf{q}}$ and $a_{\mathbf{q}}^\dagger$ are phonon annihilation and creation operators, and $\hat{J}(\mathbf{q})$ is the Fourier transform of the electron density operator:

$$\hat{J}(\mathbf{q}) = \sum_{\mathbf{r}} \sum_{\mathbf{r}'} c_{\mathbf{r}}^\dagger c_{\mathbf{r}'} e^{i\mathbf{q} \cdot (\mathbf{r} - \mathbf{r}')} \quad (6)$$

where \mathbf{r} and \mathbf{r}' are indices of electronic states/modes, $c_{\mathbf{r}}$ and $c_{\mathbf{r}}^\dagger$ are electronic annihilation and creation operators for the \mathbf{r} -mode, while $\psi_{\mathbf{r}}(\mathbf{r})$ are mode functions. For our two-donor (or double-dot) situation, where we are only interested in the two lowest energy single-electron eigenstates, we can choose them as the basis (so that \mathbf{r} and \mathbf{r}' take the value of $+$ and $-$ as defined below) and the electron-phonon coupling Hamiltonian is conveniently written in this quasi-two-level basis in terms of the Pauli spin matrices σ_x and σ_z (where spin up and down states refer to the two electronic eigenstates):

$$\begin{aligned} H_{\text{ep}} &= D \sum_{\mathbf{q}} \frac{\hbar}{2mV} \sum_{\mathbf{q}}^{\mathbf{1=2}} \hat{J}(\mathbf{q}) (A_{\mathbf{r}^+} \sigma_x + A_{\mathbf{r}^-} \sigma_z) (a_{\mathbf{q}} + a_{\mathbf{q}}^\dagger); \\ A_{\mathbf{r}^+} &= \hbar \sum_{\mathbf{r}} e^{i\mathbf{q} \cdot \mathbf{r}} \psi_{\mathbf{r}}^+; \\ A_{\mathbf{r}^-} &= \frac{1}{2} \hbar \sum_{\mathbf{r}} e^{i\mathbf{q} \cdot \mathbf{r}} \psi_{\mathbf{r}}^+ - \hbar \sum_{\mathbf{r}} e^{i\mathbf{q} \cdot \mathbf{r}} \psi_{\mathbf{r}}^-; \end{aligned} \quad (7)$$

Here the term proportional to σ_x can lead to transition between the two electronic eigenstates and is related to relaxation; while the term proportional to σ_z only causes energy renormalization of the two electronic levels, but no state mixing, so that it only leads to pure dephasing for the electronic charge states.

We first consider a double quantum dot with one electron (which is similar to a singly ionized donor pair) in GaAs where the nondegenerate conduction band minimum occurs at the Γ point. When the two dots or donors are well separated and not strongly biased, the relevant single-electron states are

$$|+\rangle = a_A(\mathbf{r}) + b_B(\mathbf{r}); \quad |-\rangle = b_A(\mathbf{r}) - a_B(\mathbf{r}); \quad (8)$$

with $a_{A(B)}(\mathbf{r}) = \psi'(\mathbf{r} - \mathbf{R}_{A(B)}) u_0(\mathbf{r})$, where $\psi'(\mathbf{r})$ is a slowly varying envelope function, and the Bloch function at the conduction band minimum ($k = 0$ at Γ point) is equal to the periodic part $u_0(\mathbf{r})$. Though we have chosen the envelopes ψ' centered at each well to be identical, they could be different, as is generally the case for quantum dots.

The deformation potential electron-phonon coupling matrix element for relaxation between the initial unperturbed eigenstate j_i and the final eigenstate j_f is proportional to $\hbar^{-1} \langle j_f | \hat{H}_1 | j_i \rangle$, where q is the phonon wavevector. For a GaAs double donor or double dot case the matrix element is proportional to

$$A_r = \hbar^{-1} \langle j_f | \hat{H}_1 | j_i \rangle = \int d\mathbf{r} j_{f0}(\mathbf{r}) j_i^* e^{iq \cdot \mathbf{r}} [ab f(\mathbf{r})^2 - ab f(\mathbf{r} - \mathbf{R})^2 + (j_f^2 - j_i^2)'(\mathbf{r})'(\mathbf{r} - \mathbf{R})] : \quad (9)$$

For small energy splittings between the states, all terms in the integrand of Eq. (9) are slowly varying functions in the interatomic spacing scale, except $j_{f0}(\mathbf{r}) j_i^*$, which is periodic and normalized in a primitive cell of the host material: $\frac{1}{R} \int d\mathbf{r} j_{f0}(\mathbf{r}) j_i^* = 1$ where R is the volume of the primitive cell. This allows for the approximation $\int d\mathbf{r} j_{f0}(\mathbf{r}) j_i^* f(\mathbf{r})$ valid for slowly varying $f(\mathbf{r})$, to be applied to (9), leading to:

$$A_r = (ab - ab e^{iq \cdot \mathbf{R}}) \int d\mathbf{r} e^{iq \cdot \mathbf{r}} [f(\mathbf{r})^2 + (j_f^2 - j_i^2)'(\mathbf{r})'(\mathbf{r} - \mathbf{R})] : \quad (10)$$

Here the first integral is an on-site contribution modulated by the phase difference $e^{iq \cdot \mathbf{R}}$ between the two dots/donors, while the second integral is a two-dot contribution that is generally much smaller because of the small overlap.

The dephasing matrix element A_r can be similarly calculated and the result is

$$A_r = i \int d\mathbf{r} [j_f^2 - j_i^2] e^{iq \cdot \mathbf{r}} \sin \frac{q \cdot \mathbf{R}}{2} \int d\mathbf{r}' e^{iq \cdot \mathbf{r}'} [f(\mathbf{r})^2 + (ab + ab) \int d\mathbf{r}'' e^{iq \cdot \mathbf{r}''} f(\mathbf{r})'(\mathbf{r} - \mathbf{R})] : \quad (11)$$

Notice that here the prefactors $j_f^2 - j_i^2$ and $ab + ab$ are for on-site and off-site integrals, just the opposite to what we have in Eq. (10). In other words, when $j_f = j_i$, A_r is small, charge decoherence caused by electron-phonon interaction is dominated by relaxation;^{31,34} when j_f and j_i are very different (so that, for example, $j_f = 1$ and $j_i = 0$), charge decoherence is dominated by pure dephasing.³⁴ Below we will focus on the relaxation matrix element $A_r = \hbar^{-1} \langle j_f | \hat{H}_1 | j_i \rangle$ as the contributing integrals are identical in the dephasing matrix element A_r .

We now consider a singly ionized phosphorus donor pair in Si, taking into account the Si band structure. For two donors not too close to each other, and possibly detuned by an axially aligned electric field, the lowest energy single-electron states are superpositions of ψ_A centered at R_A [given in Eq. (2)] and ψ_B centered at R_B , similar to Eq. (8):

$$\psi = a \psi_A(\mathbf{r}) + b \psi_B(\mathbf{r}); \quad \psi' = b \psi_A(\mathbf{r}) - a \psi_B(\mathbf{r}); \quad (12)$$

where the superposition coefficients a and b are of course not to be confused with the effective Bohr radii. If we choose $R_A = 0, R_B = R$, and ψ_i as the initial and final states, the relaxation matrix element A_r can be written as

$$\hbar^{-1} \langle j_f | \hat{H}_1 | j_i \rangle = \int d\mathbf{r} u(\mathbf{r}) u(\mathbf{r}) e^{i(\mathbf{k} - \mathbf{k} - \mathbf{q}) \cdot \mathbf{r}} [ab F(\mathbf{r}) F(\mathbf{r}) + ab F(\mathbf{r} - \mathbf{R}) F(\mathbf{r} - \mathbf{R}) e^{i(\mathbf{k} - \mathbf{k} - \mathbf{q}) \cdot \mathbf{R}} + j_f^2 F(\mathbf{r}) F(\mathbf{r} - \mathbf{R}) e^{i\mathbf{k} \cdot \mathbf{R}} - j_i^2 F(\mathbf{r}) F(\mathbf{r} - \mathbf{R}) e^{i\mathbf{k} \cdot \mathbf{R}}] : \quad (13)$$

If the energy splitting for the two double donor states is small (because of large inter-donor separations or valley interference), the dominant electron-phonon coupling is restricted to the regime of $j_f = j_i$. A simpler form of Eq. (13) can then be obtained by just keeping those integrals with $j_f = j_i$ (other integrals have fast oscillatory integrands and are thus vanishingly small):

$$\hbar^{-1} \langle j_f | \hat{H}_1 | j_i \rangle = (ab - ab e^{iq \cdot \mathbf{R}}) \int d\mathbf{r} e^{iq \cdot \mathbf{r}} F^2(\mathbf{r}) + (j_f^2 - j_i^2) \int d\mathbf{r} e^{iq \cdot \mathbf{r}} F(\mathbf{r}) F(\mathbf{r} - \mathbf{R}) \cos(\mathbf{k} \cdot \mathbf{R}) : \quad (14)$$

Equation (14) for double donor state in Si takes on quite similar form as Eq. (10) for double dot states in GaAs, with the first sum in Eq. (14) containing on-site contributions, and the second sum containing off-site (inter-dot) contributions. Thus the first sum should generally outweigh the second even for $a \neq b$. However, if one of the coefficients a or b is very small, for example due to electric field bias, the second sum may become dominant for the relaxation matrix element. However, as we mentioned above, in that situation pure dephasing becomes the more important decoherence channel. In the case when the overlap integrals do make non-negligible contributions (for example, when the two donors are detuned but not too strongly so, and the two donors are sufficiently close so that the overlap integrals are not vanishingly small), it is interesting to note that each of the terms in the sum over the valleys is multiplied by the same $\cos(k \cdot R)$ factors which appear in Eq. (4). The effect again is to have results for the off-site contribution to the electron-phonon coupling strongly oscillatory as a function of the interdonor relative position R . The average overall effect, as illustrated in Fig. 2, is to reduce the absolute value of the relaxation coupling.

We now consider the possible contributions when $|j - j'|$ may not be negligibly small. Indeed, in Si, for $\hbar\omega_q \approx 5$ meV, $q \approx 0.1 \frac{2\pi}{a}$. Thus, if the energy splitting between states is > 5 meV, we need to include in our calculation phonon wave vectors that may couple to the periodic part of the Bloch functions as described below.³⁵ Expanding the periodic part of the Bloch functions u in terms of plane waves (restricted to the reciprocal lattice wave vectors) yields:

$$u(r) = \sum_G C_G e^{iG \cdot r};$$

so that the relaxation matrix elements of Eq. (13) become

$$\begin{aligned} \hbar^{-1} \langle j' | \hat{H}^{iq} | j \rangle + i = & \sum_{G, K} \sum_{\mathbf{r}} C_G C_K \int d\mathbf{r} e^{i(G + K - k - q) \cdot \mathbf{r}} \\ & \int d\mathbf{r} e^{iG \cdot \mathbf{r}} \langle j' | F(\mathbf{r}) F(\mathbf{r}) | j \rangle = \sum_{\mathbf{r}} \langle j' | F(\mathbf{r}) F(\mathbf{r}) | j \rangle e^{i(k - k') \cdot \mathbf{r}} \\ & \int d\mathbf{r} e^{iG \cdot \mathbf{r}} \langle j' | F(\mathbf{r}) F(\mathbf{r}) | j \rangle e^{iK \cdot \mathbf{r}} + \int d\mathbf{r} e^{iK \cdot \mathbf{r}} \langle j' | F(\mathbf{r}) F(\mathbf{r}) | j \rangle e^{iG \cdot \mathbf{r}} : \end{aligned} \quad (15)$$

Since $|j - j'|$ is always relatively close to zone center (i.e., $|j - j'|$ is always much smaller than $2\pi/a$), the largest contribution to Eq. (15) comes from terms with $\mathbf{r} = 0$ and $K = G$. These are the same terms that determine the matrix elements in the small q limit, as given by Eq. (14). The important question now is whether other terms will also contribute significantly when $|j - j'|$ is not particularly close to the zone center. Recall that more than 90% of the spectral weight in u comes from a few plane waves²⁸ (the rest of the C_G coefficients are at least one order of magnitude smaller): For u_x , these are $G_x = 0; \frac{2\pi}{a}(-1; 1; 1)$, so that $k + G_x \approx 0.85 \frac{2\pi}{a}; \frac{2\pi}{a}(0.15; 1; 1)$ are the few smallest wave vectors contributing to the Bloch function $u_x(r) e^{ik_x \cdot r}$. There is thus one scenario when $G + k - K - k - q$ might have similar amplitude as q : when $\mathbf{r} = 0$ and $G - K$ is parallel to k . For example, for $q = q\hat{x}$, there are terms with $G_x + k_x - K_x - k_x = \frac{2\pi}{a}(0.3; 0; 0)$. Since these wave vectors correspond to wavelengths of the order of 15 Å, while the donor effective Bohr radius is about 20 Å, one needs to carefully evaluate the integrals involving these terms as their oscillatory integrands have the same length scale as the envelopes. The $\mathbf{r} = 0$ contribution to the electron-phonon coupling matrix elements takes the form (taking into consideration that $F = F^*$, $k = k^*$, and $\mathbf{r} = 0$):

$$\begin{aligned} \hbar^{-1} \langle j' | \hat{H}^{iq} | j \rangle + i = & \sum_{\mathbf{r}} \sum_{\mathbf{r}'} \sum_{\mathbf{r}''} C_G C_K \int d\mathbf{r} e^{i(G + K - k - q) \cdot \mathbf{r}} \\ & \int d\mathbf{r} e^{iG \cdot \mathbf{r}} \langle j' | F(\mathbf{r}) F(\mathbf{r}) | j \rangle = \sum_{\mathbf{r}} \langle j' | F(\mathbf{r}) F(\mathbf{r}) | j \rangle e^{i(k - k') \cdot \mathbf{r}} \\ & \int d\mathbf{r} e^{iG \cdot \mathbf{r}} \langle j' | F(\mathbf{r}) F(\mathbf{r}) | j \rangle e^{iK \cdot \mathbf{r}} + \int d\mathbf{r} e^{iK \cdot \mathbf{r}} \langle j' | F(\mathbf{r}) F(\mathbf{r}) | j \rangle e^{iG \cdot \mathbf{r}} : \end{aligned} \quad (16)$$

For each \mathbf{r} , only the 5 dominant G contributions mentioned previously are included in the second summation above. (As an example, in Table I we list data²⁸ for $\mathbf{r} = x$). For each $G \neq 0$, there exists one and only one K for which the exponent $G + k - K - k$ is small. If $G = 0$, all exponents are large so that the integrals should not be important in the sum in Eq. (16). Without loss of generality, we consider the $\mathbf{r} = x$ part of the sum, where $G_x + k_x - K_x - k_x = \frac{2\pi}{a}(0.3; 0; 0)$. Notice that this exponent is independent of which G_x is in consideration. Therefore, all the terms except $C_G C_K$ can be factored out of the sum over G and K , so that the sum in

Eq. (16) is proportional to $\sum_{\mathbf{G}, \mathbf{K}} C_{\mathbf{G}} C_{\mathbf{K}}$, which vanishes due to the symmetry of Si lattice, as illustrated in Table I. Therefore, for intermediate \mathbf{q} the lowest order correction to the small \mathbf{q} electron-phonon coupling matrix element vanishes, so that Eq. (14) is valid in both small and intermediate \mathbf{q} regimes for the phonons involved.

\mathbf{G}_x	0	(-1,1,1)	(-1,1,-1)	(-1,-1,1)	(-1,-1,-1)
$C_{\mathbf{G}_x}$	(0.343,0)	(-0.313, +0.313)	(-0.313, -0.313)	(-0.313, -0.313)	(-0.313, 0.313)
\mathbf{K}_x	0	(1,1,1)	(1,1,-1)	(1,-1,1)	(1,-1,-1)
$C_{\mathbf{K}_x}$	(0.343,0)	(-0.313, -0.313)	(-0.313, 0.313)	(-0.313, 0.313)	(-0.313, -0.313)
$C_{\mathbf{G}_x} C_{\mathbf{K}_x}$	(0.118,0)	(0,0.196)	(0,-0.196)	(0,-0.196)	(0,0.196)

TABLE I: Here we give the 5 most important expansion coefficients for the periodic part of the Bloch state $\psi_{\mathbf{G}_x}$ and $\psi_{\mathbf{K}_x}$ [for example, $\psi_{\mathbf{G}_x}(\mathbf{r}) = \sum_{\mathbf{G}_x} C_{\mathbf{G}_x} e^{i(\mathbf{G}_x + \mathbf{k}_x) \cdot \mathbf{r}}$].²⁸ Notice that $C_{\mathbf{G}_x}$ and $C_{\mathbf{K}_x}$ are complex in general.

In summary, the electron-phonon coupling for a P_2^+ molecular ion in Si formally behaves very similarly to that for a single electron trapped in a GaAs double quantum dot (restricted to the deformation interaction). The more complicated multi-valley bandstructure of Si and the strong inter-valley coupling introduced by the phosphorus donor atoms do not cause significant changes in the electron-phonon coupling matrix elements. The only valley interference effect occurs when the overlap between the two donors is not negligible. Even then the interference among the valleys only causes oscillatory suppression of the on-site contributions, which are relatively small anyway. Therefore, available estimates^{31,34} of decoherence induced by electron-phonon coupling based on a single-valley hydrogenic approximation in the P_2^+ system in Si should be valid. In other words, the multi-valley quantum interference effect does not provide any particular advantage (or disadvantage) for single qubit decoherence in the SiP donor charge-based quantum computer architecture.

IV. DISCUSSION AND SUMMARY

We have so far explored the feasibility of charge qubits based on the P_2^+ system in Si. We find that this system possesses decoherence properties (induced by electron-phonon coupling) similar to a GaAs double quantum dot. The Si bandstructure does, however, significantly (and adversely) influence the tunnel coupling between the two phosphorus donors, so that for many relative positions between the donors in a pair, the tunnel coupling becomes quite small. In other words, if two donors are randomly placed in a Si host, keeping their distance approximately constant, the tunnel coupling between the donor sites can vary over a wide range of values (peaked around zero) because of the Si conduction band valley degeneracy. This is obviously rather bad news for charge qubits in the P_2^+ system in Si: It implies that a large percentage of the fabricated charge qubits are unlikely to work properly since energy splitting in these two-level systems is essential for quantum computation.

The quasi-randomness of tunnel coupling in a P_2^+ donor molecular ion in Si can be contrasted with the corresponding tunnel coupling in a double QD in GaAs (or Si). The Coulomb potential of a donor provides a natural strongly localized confinement potential. Thus donors are really identical quantum dots, with fixed positions given by the donor nuclei, a fixed effective Bohr radius, and a fixed ground state energy level relative to the conduction band edge. All donor qubits are therefore expected to have identical properties except for the donor positioning problem. The main problem with donors in Si is that they break the local translational symmetry and introduce a strong valley-orbit coupling. Donor electron states are therefore superpositions of Bloch states from all the conduction band edges. The valley interference effects are thus strong in a donor system such as SiP, leading to the atomic scale oscillations in two-electron exchange studied before^{21,22} and single-electron tunneling studied here. On the other hand, a gated QD is a truly artificial atom, whose position, shape, size, and energy levels are all determined by the applied gate potentials on the metallic gates some 100 nm away. The confinement produced by gate potentials are generally quite smooth and shallow, and the barriers between potential minima are quite broad. These slowly varying features of gated QDs dictate that quantum dot electronic properties are very sensitive to the tuning of applied gate potentials. It is also inevitable that two QDs are never identical even after careful calibration.

As a simple illustration of the effect of uneven dots, we present in Fig 3 the dependence of tunnel coupling between a double QD as a function of inter-dot distance. We find that a 5% dot size variation leads to a 10 to 20% difference in the tunnel coupling. Note that, in addition to size variation, there will be inevitable fluctuations in inter-dot separations and barrier heights as well, leading to qubit fluctuations. Obviously, careful calibration is imperative for a QD system to work as a reliable charge qubit. In contrast, for donor-based charge qubits, one does not need to be concerned with such dot size variation problems since all P donors are identical.

In short, both donors in Si and gated QDs in either GaAs or Si pose difficult challenges to solid state quantum

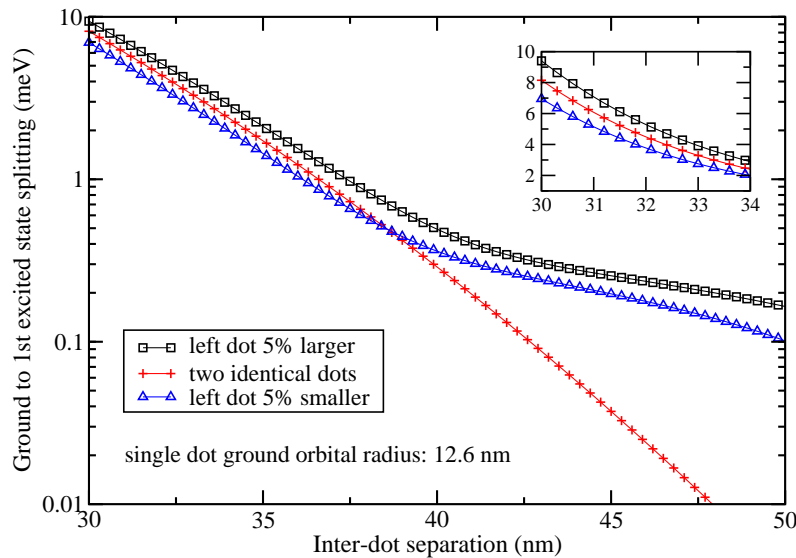


FIG. 3: (color online) Energy gap between the ground and first excited states of a single electron double dot as a function of inter-dot distance. The crosses are for two identical dots with a fixed Gaussian confinement³⁶ (with a ground orbital radius of 12.6 nm); the squares are for situations where one dot is 5% larger; the triangles are for situations where that same dot is 5% smaller. At larger inter-dot distances the different-dot configurations have larger energy splittings because the dot size difference introduces an energy level detuning that is larger than the tunnel coupling. The inset plots the same data in the range of 30 to 34 nm inter-dot distance in the linear scale, where we find that the 5% dot size variation leads to a 10 to 20% difference in the tunnel coupling.

information processing. For donors the challenge lies more on the fabrication process, while for gated dots the challenge lies more on the gating control. Which type of electron confinement (carefully calibrated gated dots or carefully positioned donors) may turn out to be better suited for quantum computing will ultimately be determined by experimental work.

For electron decoherence we have so far limited ourselves to electron-phonon coupling. As we mentioned before, for charge degrees of freedom another important source of decoherence is the fluctuation in charge traps close to a charge qubit.^{13,24,37,38} Since charge fluctuation noise can be treated in a very similar fashion as the electron-phonon coupling,¹³ we do not anticipate any significant qualitative difference between the SiP system and GaAs quantum dots. Furthermore, since electron-phonon coupling is intrinsic, the consequent decoherence is the limit that cannot be improved by having better materials and fabrication quality.

In conclusion, we show that the inter-valley quantum interference leads to a strong suppression of qubit fidelity in P_2^+ charge qubits in Si, as small nanometer-scale fluctuations in donor positioning within the Si unit cell produce an essentially random distribution (peaked around zero) in the energy separation between the two levels defining the charge qubit. We find decoherence properties of charge qubits to be qualitatively unaffected by multi-valley effects. For QD-based charge qubits, we find variations in qubit properties arising from fluctuations in dot sizes and separations, which will have to be carefully characterized individually.

Acknowledgments

This work is supported by NSA, ARDA, ARO, and LPS at the University of Maryland, by NSA, ARDA, and ARO at the University at Buffalo, and by Brazilian agencies CNPq, FUBJ, FAPERJ, PRONEX-MCT, and Instituto de Matemática e Nanociências-CNPq.

¹ X. Hu, *arXiv: cond-mat/0411012* (2004).

² S. Das Sarma, R. de Sousa, X. Hu, and B. Koiller, *arXiv: cond-mat/0411755* (2004), to be published in *Solid State Communications*.

³ D. Loss and D. P. DiVincenzo, *Phys. Rev. A* **57**, 120 (1998).

- ⁴ B. E. Kane, Nature 393, 133 (1998).
- ⁵ R. Vrijen, E. Yablonovitch, K. Wang, H. W. Jiang, A. Balandin, V. Roychowdhury, T. Mor, and D. D. Divincenzo, Phys. Rev. A 62, 012306 (2000).
- ⁶ A. Imamoglu, D. D. Awschalom, G. Burkard, D. P. Divincenzo, D. Loss, M. Sherwin, and A. Small, Phys. Rev. Lett. 83, 4204 (1999).
- ⁷ B. E. Kane, Fortschr. Phys. 48, 1023 (2000).
- ⁸ A. A. Larionov, L. E. Fedichkin, and K. A. Valiev, Nanotechnology 12, 536 (2001).
- ⁹ A. J. Skinner, M. E. Davenport, and B. E. Kane, Phys. Rev. Lett. 90, 087901 (2003).
- ¹⁰ X. Hu and S. Das Sarma, Phys. Stat. Sol. (b) 238, 360 (2003).
- ¹¹ D. Rugar, R. Budakian, H. J. Mamin, and B. W. Chui, Nature 430, 329 (2004).
- ¹² J. Elzerman, R. Hanson, L. H. W. van Beveren, B. Witkamp, L. M. K. Vandersypen, and L. P. Kouwenhoven, Nature 430, 431 (2004).
- ¹³ Y. Makhlin, G. Schon, and A. Schnirman, Rev. Mod. Phys. 73, 357 (2000).
- ¹⁴ Y. Nakamura, Y. A. Pashkin, and J. S. Tsai, Nature 398, 786 (1999).
- ¹⁵ A. Barenco, D. Deutsch, A. Ekert, and R. Jozsa, Phys. Rev. Lett. 74, 4083 (1995).
- ¹⁶ A. K. Ekert and R. Jozsa, Rev. Mod. Phys. 68, 733 (1996).
- ¹⁷ T. Tanamoto, Phys. Rev. A 61, 022305 (2000).
- ¹⁸ M. S. Sherwin, A. Imamoglu, and T. Montroy, Phys. Rev. A 60, 3508 (1999).
- ¹⁹ L. C. L. Hollenberg, A. S. Dzurak, C. J. Wellard, A. R. Hamilton, D. J. Reilly, G. J. Milburn, and R. G. Clark, Phys. Rev. B 69, 113301 (2004).
- ²⁰ L. C. L. Hollenberg, C. J. Wellard, C. I. Pakes, and A. G. Fowler, Phys. Rev. B 69, 233301 (2004).
- ²¹ B. Koiller, X. Hu, and S. Das Sarma, Phys. Rev. Lett. 88, 027903 (2002).
- ²² B. Koiller, X. Hu, and S. Das Sarma, Phys. Rev. B 66, 115201 (2002).
- ²³ B. E. Cole, J. B. Williams, B. T. King, M. S. Sherwin, and C. R. Stanley, Nature 410, 60 (2000).
- ²⁴ T. Hayashi, T. Fujisawa, H. D. Cheong, Y. H. Jeong, and Y. Hirayama, Phys. Rev. Lett. 91, 226804 (2003).
- ²⁵ J. C. Slater, Quantum Theory of Molecules and Solids, vol. 1 (McGraw-Hill, New York, 1963).
- ²⁶ W. Kohn, Solid State Physics Series, vol. 5 (Academic Press, 1957), edited by F. Seitz and D. Turnbull, p 257, and references therein.
- ²⁷ Here we consider unstrained Si, thus the nondegenerate A_1 ground state corresponds to all $p_x = p_y = p_z = 0$. The valley populations change²² when strain is applied to the sample.
- ²⁸ B. Koiller, R. B. Capaz, X. Hu, and S. Das Sarma, Phys. Rev. B 70, 115207 (2004).
- ²⁹ S. R. Schoenfeld, N. J. Curson, M. Y. Simmons, F. J. Rue, T. Hallam, L. Oberbeck, and R. G. Clark, Phys. Rev. Lett. 91, 136104 (2003).
- ³⁰ M. A. Nielsen and I. L. Chuang, Quantum Computation and Quantum Information (Cambridge, Cambridge, 2000).
- ³¹ S. D. Barrett and G. J. Milburn, Phys. Rev. B 68, 155307 (2003).
- ³² G. D. Mahan, Many-Particle Physics (Plenum, New York, 1981).
- ³³ G. Bastard, Wave mechanics applied to semiconductor heterostructures (Halsted, New York, 1988).
- ³⁴ L. Fedichkin and A. Fedorov, Phys. Rev. A 69, 032311 (2004).
- ³⁵ Calculation of pure dephasing rate is not constrained by energy conservation because pure dephasing processes do not involve energy transfer.³⁹ Therefore higher-energy phonons should also contribute to the total dephasing rate (although electron-phonon coupling matrix elements become smaller as $\hbar\omega$ increases), so that validity of the envelope function simplifications employed in the present study becomes questionable and a direct numerical calculation may be necessary.
- ³⁶ X. Hu and S. Das Sarma, Phys. Rev. A 61, 062301 (2000).
- ³⁷ Y. Nakamura, Y. A. Pashkin, T. Yamamoto, and J. S. Tsai, Phys. Rev. Lett. 88, 047901 (2002).
- ³⁸ T. Itakura and Y. Tokura, Phys. Rev. B 67, 195320 (2003).
- ³⁹ L. M. Duan and G. C. Guo, Phys. Rev. A 57, 737 (1998).